Object Based Image Analysis Technique for Distinguishing Tropical Native Forest from Plantations: A Landcover Classification Analysis of Patches Surrounding the Serra do Brigadeiro State Park, Minas Gerais, Brazil

by

Kelly Meehan

Dr. Jennifer Swenson, Adviser

04.13.16

Masters project proposal submitted in partial fulfillment of the

requirements for the Master of Environmental Management degree in

the Nicholas School of the Environment of

Duke University

1. **Introduction**

1.1 The Brazilian Atlantic Forest and Fragmentation

Today, tropical forests are extremely threatened regions, vulnerable to high levels of deforestation. A recent study assessing global forest change found that tropical forests were the only region characterized by a statistically significant increasing trend in annual forest loss over time, calculated at 2101 km^2/year (Hansen et al. 2013). The Brazilian Atlantic forest is one such forest, comprised of 1,481,946 km^2, or 17.4% of Brazil's land area (Metzger 2009). This region is regarded as one of the top five biodiversity hotspots in the world, owing to the high number of endemic species that it harbors in spite of the historical habitat loss that it has faced (Myers et al. 2000). Currently, it is estimated that only 11.73% of the Brazilian Atlantic forest's original vegetation remains (Ribeiro et al. 2009).

Further compounding the Brazilian Atlantic forest's deleterious habitat loss is the increasing fragmentation of its forest landscape. Today, more than 70% of the world's forests are within 1 km of the forest edge; yet, this rate is higher in the Atlantic forest region, with 91% of remaining forest being within 1 km of forest edge (Haddad et al. 2015). Fragmentation per se, as defined by Fahrig (2003), can result in loss of species, decrease in species richness, decline in ecosystem function (Haddad et al. 2015), and increase in tree mortality (Laurance et al. 2000). The negative effects of fragmentation on habitat patches are likely to be exacerbated by climate change in the future (Krosby et al. 2010).

1.3 Study Area

This study seeks to support the conservation efforts of the Iracambi Research and Conservation Center, located in the Brazilian Atlantic Forest. Iracambi is located in the south-eastern part of the state of Minas Gerais. The study area for this project is the nine county region surrounding the Serra do Brigadeiro, a protected state park neighboring Iracambi (Figure 1).

1.4 Remote Sensing in Tropical Areas

Land cover/land use change has been regarded as the most significant type of global change affecting ecological systems (Vitousek 2007). Today, satellite remote sensing can be used to produce thematic maps to represent land surfaces and monitor land use change (Chuvieco and Huete 2010). An example of one such application is a recent landmark study by Hansen et al. in 2013, which provided the first globally-consistent analysis of fine resolution forest cover change (Petersen et al. 2016). While the Hansen et al. analysis is a ground-breaking study that has provided free online access of its forest cover change outputs, one limitation of this dataset is that native forests are not distinguished from plantations (Tropek et al. 2014). The ability to be able to distinguish between these two is essential for assessing the ecological priority of patches since plantations cannot support the same levels of biodiversity as true forests (Fagan et al. 2015). Developing land cover classifications of tropical areas using remote sensing data is a challenging task since it is often difficult to distinguish woody landcover types with similar spectral signatures (Cordero-Sancho and Sader 2007).

1.5 Monitoring Forest Plantations in Brazil

Eucalyptus tree species are native to Australia and Indonesia and have been grown effectively in many other countries, most notably those in the tropics (Stanturf et al. 2013). While forest plantations can serve an important role in supplying high-demand timber products and providing economic opportunities to countries with fewer economic resources (Carle and Holmgren 2008), these economic benefits must be considered along with the ecological services lost when replacing native forest (Petersen et al. 2016).

Eucalyptus tree plantations in the Atlantic Forest have been shown to have significantly lower levels of species richness compared with native forests (Fonseca et al. 2009). For example, a study on bird diversity and abundance in the Atlantic Forest concluded that *Eucalyptus* plantations had only eight of the 111 species found in a neighboring native forest reserve (Marsden et al. 2001). A comparable

study found low bird diversity in the other two main tree plantation types in the Atlantic Forest: Araucaria and pine (Zurita et al. 2006). Other planted forest types, such as palm oil plantations, have also been shown to harbor lower levels of biodiversity compared with primary or secondary forests (Savilaakso et al. 2014). Additionally, the extent of nearby native forests has been shown to have an effect on diversity with shade coco plantations in the Brazilian Atlantic Forest; decreased extent of neighboring native forest had a negative effect on species richness within plantations (Faria et al. 2007).

The forest plantation industry in Brazil, predominantly comprised of *Eucalyptus* plantations (Figure 2), is an expanding industry. In Brazil, *Eucalyptus* plantations totaled 3.5 million ha in 2006 (Piketty et al. 2009) and reached 7.6 million ha by 2013 (ABRAF 2014). The greatest area of *Eucalyptus* plantations in Brazil is located in the state of Minas Gerais (ABRAF 2014) (Table 1), where the Iracambi Research and Conservation Center is located.

1.5 Research objectives

It is the goal of this study to develop a supervised classification technique utilizing RapidEye data in object-based image analysis classification that accurately distinguishes *Eucalyptus* plantations from native forest patches. The development of a RapidEye-based OBIA classification methodology to separate *Eucalyptus* plantations from native forests could be helpful to forest monitoring projects. For example, Brazil's recent decline in deforestation rates between 2000 and 2012 can be attributed in part to increased awareness of deforestation trends assessed from remote sensing analyses (Hansen et al. 2013). A method to accurately parse out *Eucalyptus* plantations from native forests in the Brazilian Atlantic forest could help accurately assess Brazil's deforestation trends and inform environmental policy.

In this study I looked at developing the most cost-effective technique for distinguishing native forest from plantations in the Atlantic Forest. Towards this effort, I utilized RapidEye data specifically since it is arguably the least expensive of all available high-resolution data (< 10m). While auxiliary LiDAR data

could help distinguish woody classes with similar spectral signatures (Zahidi et al. 2015), the cost of such data could preclude its use (Wulder et al. 2012). Lastly, in this study I explore the use of ENVI's Example Based Classification workflow, an Object Based Image Analysis (OBIA) method that is less cost-prohibitive than other segmentation programs such as eCognition.

The two research questions of this study are as follows:

1) Can RapidEye multi-spectral satellite imagery be used in an object-based image analysis (OBIA) classification to distinguish native forests from plantations?

2) Which OBIA algorithm/parameter/attribute combination is the most accurate in distinguishing native forest from plantations?

Other studies that have sought to distinguish *Eucalyptus* plantations from native forest have either included time-intensive methods such as change detection (le Maire et al. 2014), visual delineation (Petersen et al. 2016), or expensive hyperspectral satellite imagery (Goodwin et al. 2005).

2. Methods

2.1 Satellite imagery

2.1.1 RapidEye Satellite

The RapidEye satellite is a high-resolution (5x5 m) satellite, developed largely for the purpose of monitoring agriculture (Tyc et al. 2005). As such, RapidEye has a red-edge band that is unique to most multi-spectral satellites. Situated between the red and NIR bands, the red-edge band is sensitive to chlorophyll content and leaf canopy structure (RapidEye White Paper). It is suggested that the incorporation of the red-edge band can improve classification analysis of vegetation (Schuster *et al*. 2012).

2.1.2 Atmospheric correction

The RapidEye scene was a level 3A product and came finished with radiometric, sensor, and geometric corrections. I completed atmospheric corrections for the image in order to correct for

Rayleigh scattering, as is recommended when completing land cover classifications spanning over time (Song et al. 2001). Scenes were corrected individually in ENVI 5.2 using FLAASH (Fast Line-of-sight Atmospheric Analysis of Hypercubes). FLAASH input parameters included the following:

- Radiance Single Scale Factor: 10
- FLAASH Advanced Settings, Zentih Angle = 180-(ABS(CraftViewAngle))
- FLAASH Advanced Settings, Azimuth Angle =-(360-AzimuthAngle)+180
- Atmospheric Model: Tropical
- FLAASH ground elevation values: derived from Shuttle Radar Topography Mission (SRTM) elevation (void filled) data

2.2 OBIA Classification

There are two main types of remote sensing classification approaches: 1) single pixel-based methods and 2) object based image analysis. An OBIA approach first groups together contiguous, spectrally similar pixels, with the goal of segmenting objects into spectrally homogenous groups to use for classification (Qian Yu, Peng Gong, Nick Clinton, Greg Biging, Maggi Kelly 2006).

One problem that arises when using a pixel-based classification approach with high resolution imagery is that there is an increase in variability in spectral signatures within a class, which consequently lowers the ability to separate classes and produces a salt-and-pepper effect (Ibid). Since an OBIA approach groups spectrally similar contiguous pixels, it allows for the creation of objects that, when considered as a whole, have less local spectral variation (Ibid).

Using the Example Based Feature Extraction Workflow in ENVI 5.2, I ran 26 unique classification trials utilizing one RapidEye scene from August 13th, 2011 (Table 2). I used a unique algorithm and parameter combination for each trial in order to test which method produced the highest accuracy results.

2.2.1 OBIA Algorithms

The Example Based Feature Extraction Workflow in ENVI 5.2 offers three different classification algorithms to choose from: K-Nearest Neighbor (KNN), Support Vector Machines (SVM), and Principal Component Analysis (PCA).

With K-Nearest Neighbor, each pixel cluster is assigned to the class belonging to the training example that it is nearest to in spectral space.

Support vector machines are a promising technique for remote sensing classifications. Since the distribution of remotely sensed imagery data is often uncertain, they do not always satisfy the assumptions of commonly used parametric classification methods such as Maximum Likelihood. SVM is a non-parametric classification method; there is no assumption that the data are normally distributed (Mountrakis et al. 2011).

SVM is a statistical learning algorithm, meaning that it runs iterations in order to produce a classifier with the best results (Mountrakis et al. 2011). SVM places a hyperplane in n-dimensional space in order to separate classes. For a given classification, there could be multiple hyperplanes that could separate two classes, but SVM selects the one that has the greatest margin width; that is to say, it selects the hyperplane that is farthest away from any of the training data points (Figure 4). SVM strikes a unique balance between avoiding overfitting (and allowing some misclassified instances) and accuracy (Mountrakis et al. 2011).

SVMs are also appealing in that they can perform well with minimal training samples. Training data for remote sensing can be time intensive and costly (Mountrakis et al. 2011). The only training samples used in SVMs are the support vectors which define the hyperplane; thus, SVMs can utilize a relatively small number of samples if training samples that are close to hyperplanes regions are strategically selected (Foody and Mathur 2004). This unique capability is an important consideration because obtaining ground reference information for remote sensing data is a costly endeavor (Mountrakis et al. 2011).

In this analysis, the n-dimensional space consisted of spectral, texture, and in some cases, spatial attributes (Table 3). Training points in this case were the training polygons (30 for each class). Data samples to be classified were the remaining image polygon segments of the RapidEye image.

2.1.4 Vegetation Indices

The normalized difference vegetation index (NDVI) was calculated using equation (1) and used as ancillary data in the Feature Extraction Workflow.

$$NDVI = \frac{\text{RapidEye 5 – RapidEye 3}}{\text{RapidEye 5+ RapidEye 3}} \quad (1)$$

Where

RapidEye 5 = reflected near-infrared (760 – 850 nm)

RapidEye 3 = reflected red (630 – 685 nm)

The normalized difference red-edge (NDRE) index (RapidEye White Paper) is similar to NDVI, was calculated using equation (2) and used as ancillary data in the Feature Extraction Workflow.

$$NDRE = \frac{\text{RapidEye 5 – RapidEye 4}}{\text{RapidEye 5+ RapidEye 4}} \quad (2)$$

Where

RapidEye 5 = reflected near-infrared (760 – 850 nm)

RapidEye 4 = reflected red (690 – 730 nm)

2.1.5 OBIA Image Segmentation

The RapidEye image used in the classification trials was segmented using the same parameters for each classification. A Scale Level of five was used for the Edge Algorithm Segmentation Setting, and a Merge Level of 90 was used for the Full Lambda Schedule Algorithm Merge Setting. Segmentation and merge level values were selected based on the results of pilot trials of this study. These pilot studies suggested that the use of a small scale level and high merge level produced segments that did not group together contiguous pixels belonging to separate classes. A uniform value of three was used for the Texture Kernel Size as suggested by ENVI for complex, noisy data (Harris 2016).

2.2 Ground-reference points

In January 2015, I collected 136 ground-reference points across the study area (Figure 1). The majority of points were recorded in pasture, native forest, *Eucalyptus* plantations, and coffee plantations. A few points were also taken of dirt roads, water, urban areas, and banana and palm plantations. Approximately 60 points were collected from throughout the 8 counties; the remaining 76 points were collected from the area directly surrounding Iracambi. I used these points to train myself how to identify *Eucalyptus* plantations and native forests in both RapidEye and GoogleEarth imagery. This knowledge was used in order to create additional training areas for classifications, as well as ground reference points for completing accuracy assessments.

2.3 Classification Training Areas

I used the same training polygons for each trial. For each of the classes, I selected 30 segments to serve as training polygons. Segments were selected while viewing the area simultaneously in the RapidEye image and in the closest historical 2011 image in GoogleEarth.

2.3.1 *Eucalyptus* identification

A combination of the following criteria was used to identify each *Eucalyptus* plantation training area:

1. Extremely dark segments in true-color image display
2. Bright orange, homogenous, segments using red-edge false color RapidEye image display (NIR, red edge, red bands)
3. Bright red, homogenous, traditional false color RapidEye image display (NIR, red, blue)
4. Homogeneity and high density of crown shape in Google Imagery
5. Neat border shape
6. Evidence in Google Earth historical imagery of logging within a patch, and/or growth over time, often with earlier scenes of bare earth before planting occurred, or of recently planted trees in rows.

2.3.2 Pasture identification

A combination of the following criteria were used to identify each pasture training area:

1. Large patch area
2. Neat border patches.

3. Light green/brown true color image in RapidEye image.
4. No change present in comparing time-series in Google images.
5. Turquois-colored, homogenous, segments using red-edge false color RapidEye image display (NIR, red edge, red bands)
6. Teal-colored, homogenous, traditional false color RapidEye image display (NIR, red, blue)

2.3.3 Native forest identification

A combination of the following criteria were used to identify each native forest training area:

1. Highly irregular shape, especially compared to other classes.
2. Secropia trees (bright white spots in GoogleEarth, or bluish specks in RapidEye true color imagery display)
3. Consistent existence in GoogleEarth time series images.
4. Larger patches in high mountain regions; smaller patches in lower elevation areas.
5. Canopy has flat appearance in GoogleEarth.
6. Native patches have more shade within the patch since there is heterogeneity in canopy height.
7. Dark orange colored, heterogeneous, segments using red-edge false color RapidEye image display (NIR, red edge, red bands)
8. Dark red colored, homogenous, traditional false color RapidEye image display (NIR, red, blue)

2.4 Classification accuracy assessment

I completed an accuracy assessment for each trial classification output using the same set of 200 sample points. Following commonly accepted accuracy assessment protocol (Congalton 1991), I systematically generated the 200 points, which were equally split between native forest and *Eucalyptus* samples. The 200 points were dispersed sporadically throughout the image and were created by referencing RapidEye image, in tandem with GoogleEarth images. For each trial, I extracted the classification assignment for each of the 200 sample points and compared them to their corresponding ground-reference value. I generated a confusion matrix for each trial using the "caret" package for version 3.2.2 of the 64-bit version of R (Kuhn 2008).

3.0 Results

3.1 Accuracy Assessments

Accuracy for the 26 trials ranged from 67% to 89% (Table 2). The trial that resulted in the highest accuracy used the SVM algorithm, excluding spatial attributes, and with a threshold assignment of 800 (Figure 5).

3.2 Comparison of Models

An ANOVA comparison revealed that there was a difference in mean accuracy values between the KNN and SVM trials ($F= 13.37$, $df= 1$, $p= 0.00132$) (Figure 6). It also revealed a difference between those trials that included spatial attributes vs. those that did not ($F= 23.99$, $df= 2$, $p < 0.0001$). Results did not identify one of the four groups of trials (Figure 7) as outperforming all others. However, the KNN trials utilizing spatial attributes were statistically different from the other three groups and performed the worst.

4.0 Discussion/Conclusion

This study found that spectral separation between native forest and *Eucalyptus* was successfully accomplished utilizing an OBIA classification workflow employing a Support Vector Machine algorithm. This research is the first sensitivity analysis to assess the classification accuracy of various models utilizing RapidEye imagery, each with unique user-defined parameters seeking to distinguish native forest patches from Eucalyptus plantations. These findings are particularly pertinent for remote sensing of tropical forests in Brazil, where 90% of tree cover loss occurred not within plantations (Petersen et al. 2016).

Future research should test repeating the technique recommended here for a greater number of images. It is possible that a larger sample size of images analyzed could reveal a statistically significant difference between the four categories of approaches examined in this paper.

In light of the alarming rate of deforestation currently impacting the tropics, accurate land cover classifications of these regions are of pivotal importance.

To date, this study offers the most time-efficient, low-cost method with which to remotely distinguish *Eucalyptus* plantations from native forest utilizing high-resolution imagery. These results offer a technique that can be utilized with merely one remote sensing software package, without the use of manual delineation or time-series analysis, and independent of cost-prohibitive hyperspectral imagery or LiDAR data. Since Eucalyptus plantations are often misclassified with native forest due to their spectral signature similarity, the technique outlined in this paper can help support efforts to more accurately measure remaining forest at a pivotal point in time when global tropical forests face massive alarming deforestation rates.

Acknowledgements

I would like to sincerely thank my advisor, Professor Jennifer Swenson for her guidance throughout the course of this study. I am also deeply grateful to Robin and Binka LeBreton for their support of this project.

References

ABRAF (2014). Planted Forests in Brazil. Statistical Yearbook 2014.

Carle, J., and P. Holmgren. 2008. Wood from Planted Forests, A Global Outlook 2005-2030. Forest Products Journal 58:6–18.

Congalton, R. G. 1991. A review of assessing the accuracy of classifications of remotely sensed data. Remote Sensing of Environment 37:35–46.

Cordero-Sancho, S., and S. a Sader. 2007. Spectral analysis and classification accuracy of coffee crops using Landsat and a topographic-environmental model. International Journal of Remote Sensing 28:1577–1593.

Fagan, M. E., R. S. DeFries, S. E. Sesnie, J. P. Arroyo-Mora, C. Soto, A. Singh, P. A. Townsend, and R. L. Chazdon. 2015. Mapping species composition of forests and tree plantations in northeastern Costa Rica with an integration of hyperspectral and multitemporal landsat imagery. Remote Sensing 7:5660–5696.

Fahrig, L. 2003. Effects of Habitat Fragmentation on Biodiversity. Annual Review Of Ecology Evolution And Systematics 34:487–515.

Faria, D., M. L. B. Paciencia, M. Dixo, R. R. Laps, and J. Baumgarten. 2007. Ferns, frogs, lizards, birds and bats in forest fragments and shade cacao plantations in two contrasting landscapes in the Atlantic forest, Brazil. Biodiversity and Conservation 16:2335–2357.

Fonseca, C. R., G. Ganade, R. Baldissera, C. G. Becker, C. R. Boelter, A. D. Brescovit, L. M. Campos, T. Fleck, V. S. Fonseca, S. M. Hartz, F. Joner, M. I. Käffer, A. M. Leal-zanchet, M. P. Marcelli, A. S. Mesquita, C. A. Mondin, C. P. Paz, M. V Petry, F. N. Piovensan, J. Putzke, A. Stranz, M. Vergara, and E. M. Vieira. 2009. Towards an ecologically-sustainable forestry in the Atlantic Forest. Biological Conservation 142:1209–1219.

Foody, G. M., and A. Mathur. 2004. Toward intelligent training of supervised image classifications: Directing training data acquisition for SVM classification. Remote Sensing of Environment 93:107–117.

Goodwin, N., R. Turner, and R. Merton. 2005. Classifying Eucalyptus forests with high spatial and spectral resolution imagery: An investigation of individual species and vegetation communities. Australian Journal of Botany 53:337–345.

Haddad, N. M., L. A. Brudvig, J. Clobert, K. F. Davies, A. Gonzalez, R. D. Holt, T. E. Lovejoy, J. O. Sexton, M. P. Austin, C. D. Collins, W. M. Cook, E. I. Damschen, R. M. Ewers, B. L. Foster, C. N. Jenkins, A. J. King, W. F. Laurance, D. J. Levey, C. R. Margules, B. A. Melbourne, A. O. Nicholls, J. L. Orrock, D. Song, and J. R. Townshend. 2015. Habitat fragmentation and its lasting impact on Earth ' s ecosystems:1–9.

Hansen, M. C., P. V Potapov, R. Moore, M. Hancher, S. a Turubanova, and A. Tyukavina. 2013a. High-Resolution Global Maps of 21st-Century Forest Cover Change. Science 342:850–853.

Hansen, M. C., P. V Potapov, R. Moore, M. Hancher, S. A. Turubanova, A. Tyukavina, D. Thau, S. V Stehman, S. J. Goetz, T. R. Loveland, A. Kommareddy, A. Egorov, L. Chini, C. O. Justice, and J. R. G. Townshend. 2013b. High-Resolution Global Maps of 21st-Century Forest Cover Change. Science 342 :850–853.

Krosby, M., J. Tewksbury, N. M. Haddad, and J. Hoekstra. 2010. Ecological connectivity for a changing climate. Conservation Biology 24:1686–1689.

Kuhn, M. 2008. Building Predictive Models in R Using the caret Package. Journal Of Statistical Software 28:1–26.

Laurance, W. F., P. Delamônica, S. G. Laurance, H. L. Vasconcelos, and T. E. Lovejoy. 2000. Rainforest fragmentation kills big trees. Nature 404:836.

le Maire, G., S. Dupuy, Y. Nouvellon, R. A. Loos, and R. Hakamada. 2014. Mapping short-rotation plantations at regional scale using MODIS time series: Case of eucalypt plantations in Brazil. Remote Sensing of Environment 152:136–149.

Marsden, S. J., M. Whiffin, and M. Galetti. 2001. Bird diversity and abundance in forest fragments and Eucalyptus plantations around an Atlantic forest reserve, Brazil. Biodiversity and Conservation 10:737–751.

Metzger, J. P. 2009. Conservation issues in the Brazilian Atlantic forest. Biological Conservation 142:1138–1140.

Mountrakis, G., J. Im, and C. Ogole. 2011. Support vector machines in remote sensing: A review. ISPRS Journal of Photogrammetry and Remote Sensing 66:247–259.

Myers, N., R. A. Mittermeier, C. G. Mittermeier, G. A. B. da Fonseca, and J. Kent. 2000. Biodiversity hotspots for conservation priorities. Nature 403:853–858.

Petersen, R., D. Aksenov, E. Esipova, E. Goldman, N. Harris, I. Kurakina, T. Loboda, A. Manisha, S. Sargent, and V. Shevade. 2016. Mapping Tree Plantations with Multispectral Imagery: Preliminary Results for Seven Tropical Countries:1–18.

Piketty, M. G., M. Wichert, A. Fallot, and L. Aimola. 2009. Assessing land availability to produce biomass for energy: The case of Brazilian charcoal for steel making. Biomass and Bioenergy 33:180–190.

Qian Yu, Peng Gong, Nick Clinton, Greg Biging, Maggi Kelly, D. S. 2006. Objectbased detailed vegetation classification with airborne high spatial resolution remote sensing imagery. Photogrammetric Engineering and Remote Sensing 72:799–811.

Ribeiro, M. C., J. P. Metzger, A. C. Martensen, F. J. Ponzoni, and M. M. Hirota. 2009. The Brazilian Atlantic Forest: How much is left, and how is the remaining forest distributed? Implications for conservation. Biological Conservation 142:1141–1153.

Savilaakso, S., C. Garcia, J. Garcia-Ulloa, J. Ghazoul, M. Groom, M. R. Guariguata, Y. Laumonier, R. Nasi, G. Petrokofsky, J. Snaddon, and M. Zrust. 2014. Systematic review of effects on biodiversity from oil palm production. Environmental Evidence 3:1–20.

Song, C., C. E. Woodcock, K. C. Seto, M. P. Lenney, and S. A. Macomber. 2001. Classification and change detection using Landsat TM data: When and how to correct atmospheric effects? Remote Sensing of Environment 75:230–244.

Stanturf, J. A., E. D. Vance, T. R. Fox, and M. Kirst. 2013. Eucalyptus beyond Its Native Range: Environmental Issues in Exotic Bioenergy Plantations. International Journal of Forestry Research 2013:1–5.

Tropek, R., J. Beck, P. Keil, Z. Musilová, Š. Irena, and D. Storch. 2014. Comment on “High-resolution global maps of 21st-centry forest cover change.” Science (New York, N.Y.) 344:981.

Tyc, G., J. Tulip, D. Schulten, M. Krischke, and M. Oxfort. 2005. The RapidEye mission design. Acta Astronautica 56:213–219.

Vitousek, P. M. 2007. Beyond Global Warming: Eecology and Global Change 75:1861–1876.

Wulder, M. A., J. C. White, R. F. Nelson, E. Næsset, H. O. Ørka, N. C. Coops, T. Hilker, C. W. Bater, and T. Gobakken. 2012. Lidar sampling for large-area forest characterization: A review.

Zahidi, I., B. Yusuf, A. Hamedianfar, H. Z. M. Shafri, and T. A. Mohamed. 2015. Object-based classification of QuickBird image and low point density LIDAR for tropical trees and shrubs mapping. European Journal of Remote Sensing 48:423–446.

Zurita, G. A., N. Rey, D. M. Varela, M. Villagra, and M. I. Bellocq. 2006. Conversion of the Atlantic Forest into native and exotic tree plantations: Effects on bird communities from the local and regional perspectives. Forest Ecology and Management 235:164–173.

Appendix

Table 1. Area Occupied by *Eucalyptus* Trees in Brazil, 2006 - 2013 (Graphic by ABRAF, 2014)

STATE	AREA OCCUPIED BY EUCALYPTUS TREES (ha)							
	2006	2007	2008	2009	2010	2011	2012	2013
MINAS GERAIS	1,181,429	1,218,212	1,278,210	1,300,000	1,400,000	1,401,787	1,438,971	1,404,429
SÃO PAULO	915,841	911,908	1,001,080	1,029,670	1,044,813	1,031,677	1,041,695	1,010,444
MATO GROSSO DO SUL	119,319	207,687	265,250	290,890	378,195	475,528	587,310	699,128
BAHIA	540,172	550,127	587,610	628,440	631,464	607,440	605,464	623,971
RIO GRANDE DO SUL	184,245	222,245	277,320	271,980	273,042	280,198	284,701	316,446
ESPÍRITO SANTO	207,800	208,819	210,410	204,570	203,885	197,512	203,349	221,559
MARANHÃO	93,285	106,802	111,120	137,360	151,403	165,717	173,324	209,249
PARANÁ	121,908	123,070	142,430	157,920	161,422	188,153	197,835	200,473
MATO GROSSO[4]	113,770	114,854	132,922	147,378	150,646	175,592	184,628	187,090
PARÁ	115,806	126,286	136,290	139,720	148,656	151,378	159,657	159,657
GOIÁS[5]	98,765	102,032	113,177	115,286	116,439	118,636	115,567	121,375
TOCANTINS	13,901	21,655	31,920	44,310	47,542	65,502	109,000	111,131
SANTA CATARINA	70,341	74,008	77,440	100,140	102,399	104,686	106,588	107,345
AMAPÁ	58,473	58,874	63,310	62,880	49,369	50,099	49,506	57,169
PIAUÍ	-	-	-	-	37,025	26,493	27,730	28,053
OTHERS	27,491	31,588	27,580	28,380	4,650	9,314	18,838	15,657
TOTAL	**3,862,546**	**4,078,168**	**4,456,069**	**4,658,924**	**4,900,949**	**5,049,714**	**5,304,164**	**5,473,176**

Table 2. Trial Algorithm, Parameter, and Spatial Attribute Specifications and Accuracy Results

Trial	Attributes	Algorithm	Parameters	Accuracy
23	No Spatial	SVM	RB .02/800	89.05%
25	No Spatial	SVM	RB .02/900	88.06%
21	No Spatial	SVM	RB .02/700	87.56%
17	No Spatial	SVM	RB .02/500	86.07%
19	No Spatial	SVM	RB .02/600	86.07%
15	No Spatial	SVM	RB .02/400	85.57%
1	No Spatial	KNN	Neighbors 1	85.07%
26	With Spatial	SVM	RB .02/900	85.07%
11	No Spatial	SVM	RB .02/200	84.58%
13	No Spatial	SVM	RB .02/300	84.58%
24	With Spatial	SVM	RB .02/800	84.58%
22	With Spatial	SVM	RB .02/700	84.08%
18	With Spatial	SVM	RB .02/500	81.59%
9	No Spatial	SVM	RB .02/1000	81.09%
3	No Spatial	KNN	Neighbors 3	80.10%
20	With Spatial	SVM	RB .02/600	80.10%
16	With Spatial	SVM	RB .02/400	79.60%
14	With Spatial	SVM	RB .02/300	78.61%
5	No Spatial	KNN	Neighbors 5	77.61%
12	With Spatial	SVM	RB .02/200	76.12%
10	With Spatial	SVM	RB .02/1000	74.63%
7	No Spatial	SVM	RB .02/100	74.13%
8	With Spatial	SVM	RB .02/100	71.14%
2	With Spatial	KNN	Neighbors 1	68.66%
6	With Spatial	KNN	Neighbors 5	67.66%
4	With Spatial	KNN	Neighbors 3	67.16%

Table 3. Object features used in object based image analysis classifications (adapted from Harris, 2016).

Spectral Attributes (Computed on each band of image)	
Attribute	Description
Spectral_Mean	Mean value of pixels in segment x for band y
Spectral_Max	Maximum value of pixels in segment x for band y
Spectral_Min	Minimum value of pixels in segment x for band y
Spectral_STD	Standard deviation value value of pixels in segment x for band y
Texture Attributes*	
Attribute	Description
Texture_Range	Average data range of the pixels within the kernel**
Texture_Mean	Average value of the pixels within the kernel**
Texture_Variance	Average variance of the pixels within the kernel**
Texture_Entropy	Average entropy value of the pixels within the kernel**
	* (Computed on each band of image. Consists of two-step process whereby 1) value assigned to each pixel based on the attributes caluclated across kernel window and 2) overall value for segment determined by averaging value from Step 1 for all pixels within segment.
	** Texture Kernel Size = 3
Spatial Attributes	
Attribute	Description
Area	Total area of segment.
Length	Combined length of all boundaries in segment.
Compactness	Shape measure of compactness of segment.
Convexity	Length of convex hull/Length
Solidity	Area/area of convex hull
Roundness	Measure of comparison of polygon to a square
Form_Factor	Shape measure comparing are of polygon to square of total perimeter
Enlongation	Major_Length/Minor_Length
Rectangular_Fit	Shape measure indicating how well segment is described by a rectangle
Main_Direction	Angle subtended by the major axis of the polygon and the x-axis
Major_Length	Length of major axis of polygon
Minor_Length	Length of minor axis polygon
Number_of_Holes	Number of holes in polygon
Hole_Area/Solid_Area	Area/outer contour area

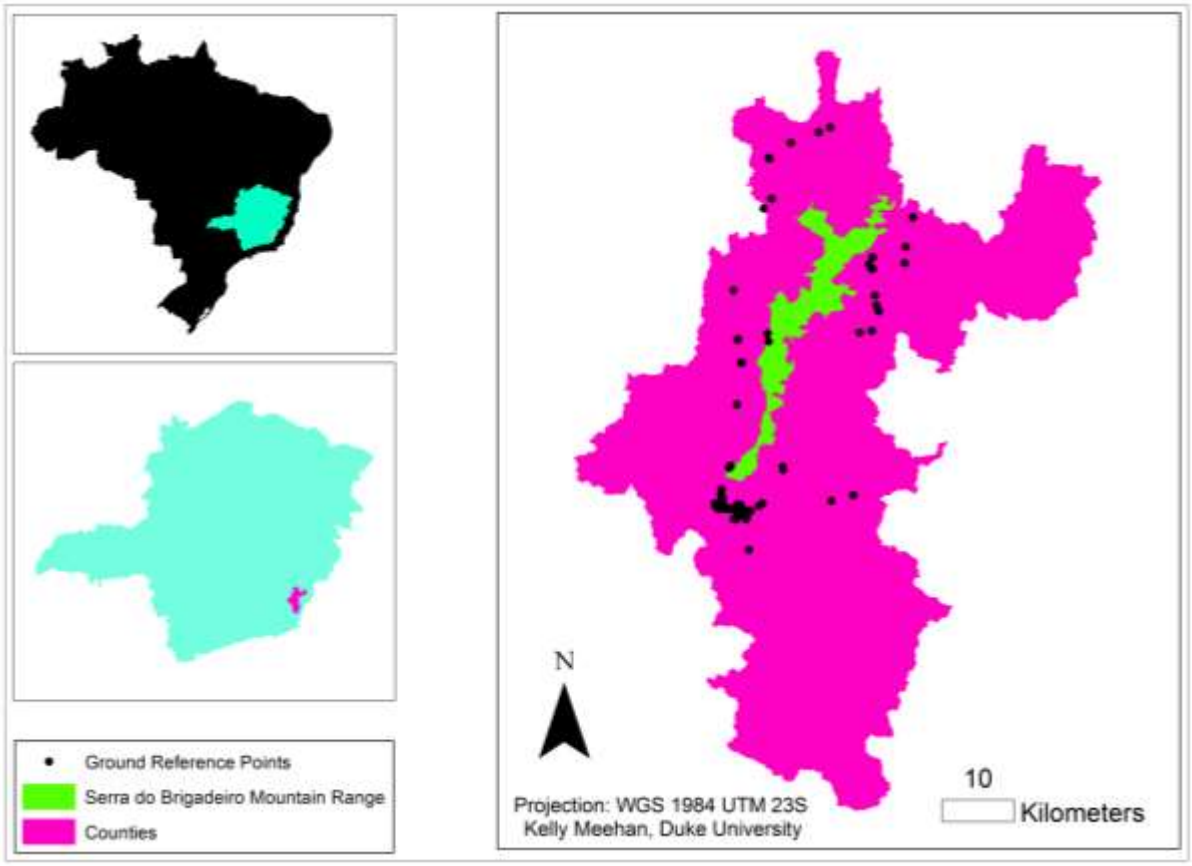

Figure 1. Ground-Reference Points collected at study area in Minas Gerais, Brazil

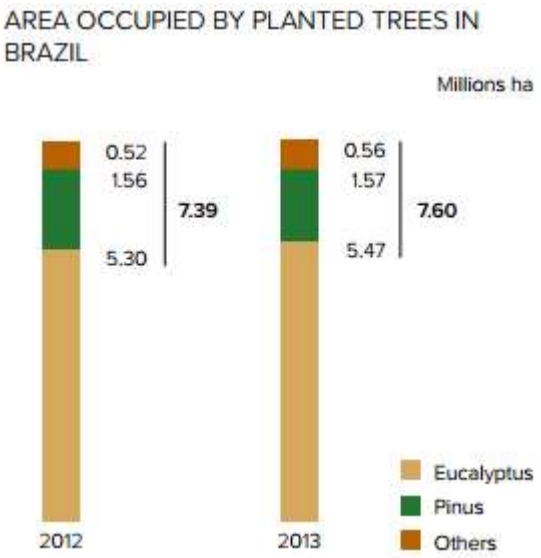

Figure 2. Area Occupied by Planted Trees in Brazil (Graphic by ABRAF, 2014)

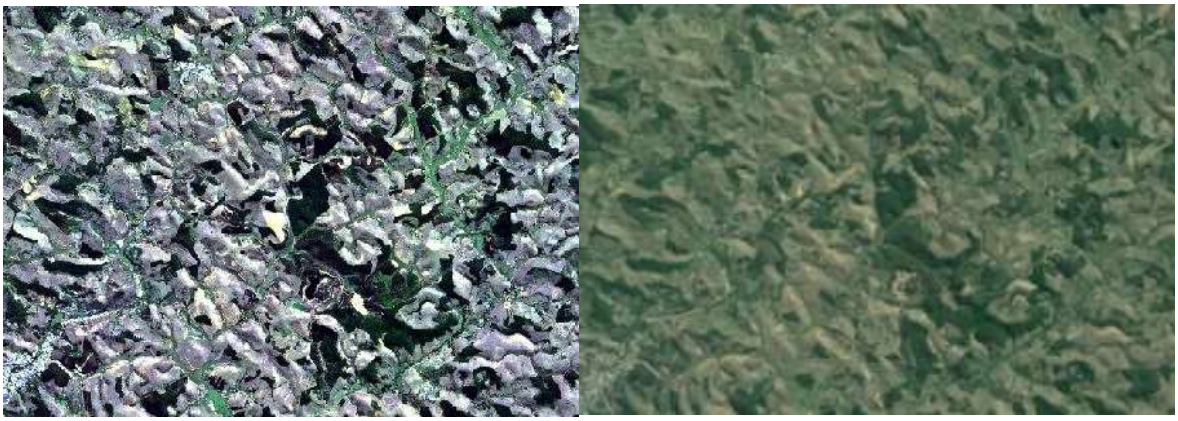

Figure 3. RapidEye image (left) with corresponding GoogleEarth image (right)

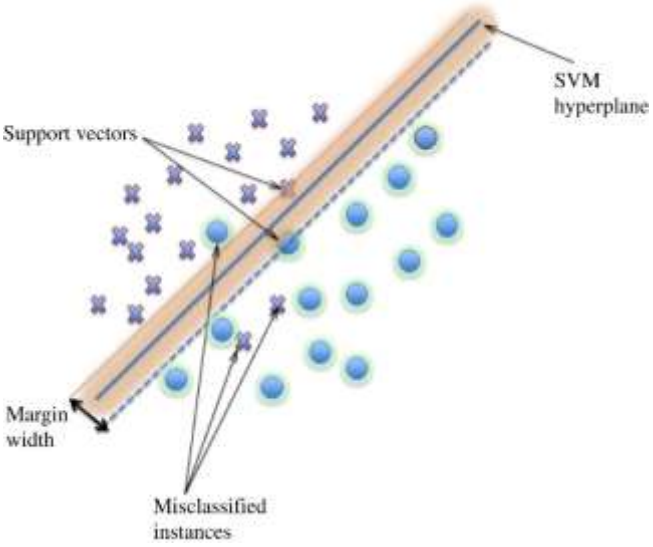

Figure 4. Example of a binary, linear Support Vector Machine (Graphic by Mountrakis et al., 2011)

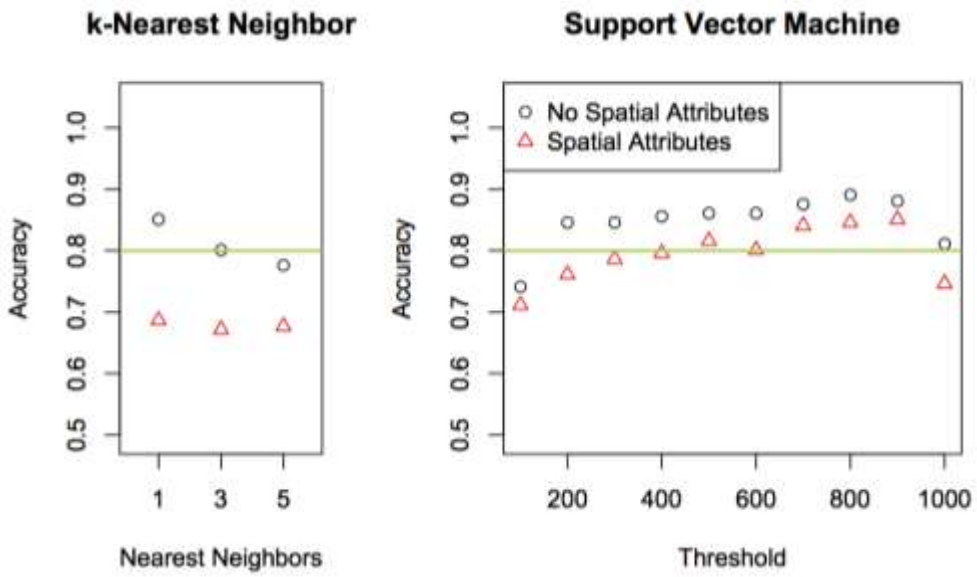

Figure 5. Accuracy Assessment Results of 26 Trials

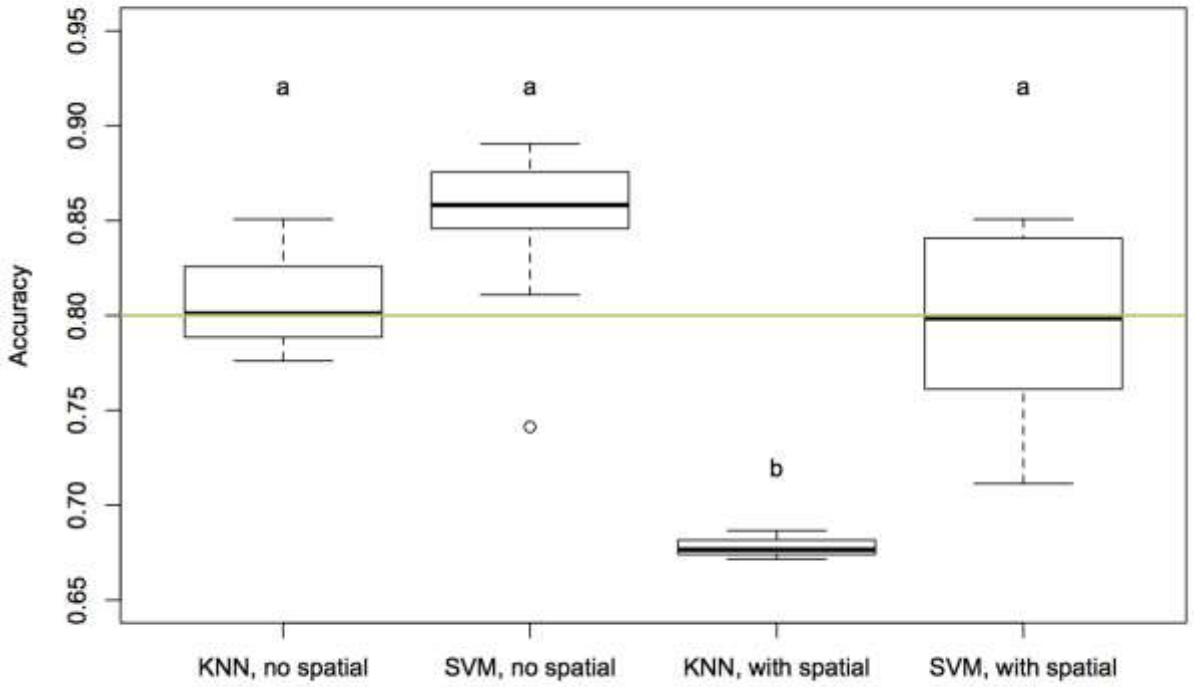

Figure 6. ANOVA results comparing four categories of classification trials.

Algorithm	Spatial Attribute Use	
	K-Nearest Neighbor (no spatial attributes)	K-Nearest Neighbor (with spatial attributes)
	Support Vector Machine (no spatial attributes)	Support Vector Machine (with spatial attributes)

Figure 7. Visualization of four types of trials completed.